Journal of the American Heart Association

ORIGINAL RESEARCH

Identification of *Prostaglandin I_2 Synthase* Rare Variants in Patients With Williams Syndrome and Severe Peripheral Pulmonary Stenosis

Ayako Chida-Nagai, MD, PhD*; Hiroyuki Akagawa, MD, PhD; Saori Sawai, MD; Yue-Jiao Ma, MD, PhD; Satoshi Yakuwa, MD, PhD; Jun Muneuchi, MD, PhD; Kazushi Yasuda, MD, PhD; Hirokuni Yamazawa, MD, PhD; Toshiyuki Yamamoto, MD, PhD; Emi Takakuwa, MD, PhD; Utano Tomaru, MD, PhD; Yoshiyuki Furutani, PhD; Tatsuya Kato, MD, PhD; Gen Harada, MD, PhD; Kei Inai, MD, PhD; Toshio Nakanishi, MD, PhD; Atsushi Manabe, MD, PhD; Atsuhito Takeda, MD, PhD; Zhi-Cheng Jing, MD, PhD*

BACKGROUND: Peripheral pulmonary stenosis (PPS) is a condition characterized by the narrowing of the pulmonary arteries, which impairs blood flow to the lung. The mechanisms underlying PPS pathogenesis remain unclear. Thus, the aim of this study was to investigate the genetic background of patients with severe PPS to elucidate the pathogenesis of this condition.

METHODS AND RESULTS: We performed genetic testing and functional analyses on a pediatric patient with PPS and Williams syndrome (WS), followed by genetic testing on 12 patients with WS and mild-to-severe PPS, 50 patients with WS but not PPS, and 21 patients with severe PPS but not WS. Whole-exome sequencing identified a rare *PTGIS* nonsense variant (p.E314X) in a patient with WS and severe PPS. Prostaglandin I_2 synthase (PTGIS) expression was significantly downregulated and cell proliferation and migration rates were significantly increased in cells transfected with the *PTGIS* p.E314X variant-encoding construct when compared with that in cells transfected with the wild-type *PTGIS*-encoding construct. p.E314X reduced the tube formation ability in human pulmonary artery endothelial cells and caspase 3/7 activity in both human pulmonary artery endothelial cells and human pulmonary artery smooth muscle cells. Compared with healthy controls, patients with PPS exhibited downregulated pulmonary artery endothelial prostaglandin I_2 synthase levels and urinary prostaglandin I metabolite levels. We identified another *PTGIS* rare splice-site variant (c.1358+2T>C) in another pediatric patient with WS and severe PPS.

CONCLUSIONS: In total, 2 rare nonsense/splice-site *PTGIS* variants were identified in 2 pediatric patients with WS and severe PPS. *PTGIS* variants may be involved in PPS pathogenesis, and PTGIS represents an effective therapeutic target.

Key Words: genetic testing ■ peripheral pulmonary stenosis ■ prostaglandin I_2 synthase ■ whole-exome sequencing ■ Williams syndrome

Peripheral pulmonary stenosis (PPS) is a form of vascular stenosis—or narrowing of blood vessels—that extends from the main pulmonary artery to the right and left pulmonary arteries and the periphery. The incidence of PPS among patients with congenital heart disease is 2% to 3%.[1] Although some

Correspondence to: Ayako Chida-Nagai, MD, PhD, Department of Pediatrics, Hokkaido University, Kita 15, Nishi 7, Sapporo, Hokkaido 060-8638, Japan. Email: ayakonagai@med.hokudai.ac.jp. Zhi-Cheng Jing, MD, PhD, Department of Cardiology, Guangdong Cardiovascular Institute, Guangdong Provincial People's Hospital, Guangdong Academy of Medical Sciences Southern Medical University, Guangzhou 510080, China. Email: jingzhicheng@gdph.org.cn

*A. Chida-Nagai and Z.-C. Jing contributed equally.

This article was sent to Jacquelyn Y. Taylor, PhD, PNP-BC, RN, FAHA, FAAN, Associate Editor, for review by expert referees, editorial decision, and final disposition.

Supplemental Material is available at https://www.ahajournals.org/doi/suppl/10.1161/JAHA.123.032872.

For Sources of Funding and Disclosures, see page 14.

JAHA is available at: www.ahajournals.org/journal/jaha

RESEARCH PERSPECTIVE

What Is New?

- This study identified rare *PTGIS* variants in 2 pediatric patients with Williams syndrome and severe peripheral pulmonary stenosis, revealing a potential association and highlighting prostaglandin I_2 synthase as a promising therapeutic target for treating peripheral pulmonary stenosis.

What Question Should Be Addressed Next?

- Subsequent investigations should aim to clarify the synergistic effect of Williams syndrome-associated 7q11.23 deletions and rare *PTGIS* variants in severe peripheral pulmonary stenosis development, and conduct further research on *PTGIS* variants in peripheral pulmonary stenosis cases without Williams syndrome to identify novel therapeutic approaches.

Nonstandard Abbreviations and Acronyms

hPAECs	human pulmonary artery endothelial cells
hPASMCs	human pulmonary artery smooth muscle cells
PAH	pulmonary arterial hypertension
PPS	peripheral pulmonary stenosis
PTGIS	prostaglandin I_2 synthase
WES	whole-exome sequencing
WS	Williams syndrome

mild PPS cases may resolve spontaneously without treatment, percutaneous transluminal angioplasty or surgical intervention is often needed to alleviate moderate PPS, which can require reintervention.[1] Moreover, treatment of severe PPS, which has a poor prognosis, is challenging. In particular, stenosis of the intrapulmonary arteries cannot be treated by surgical interventions and can lead to death.[2,3]

Severe PPS and pulmonary arterial hypertension (PAH) exhibit similar clinical characteristics. Although the lesion sites of PPS and PAH are relatively central and within small pulmonary arteries, respectively, they both increase pulmonary arterial pressure and induce right heart failure. Notably, patients initially diagnosed with PAH are commonly diagnosed with PPS upon detailed examination. Recently, various pulmonary vasodilators, including endothelin receptor antagonists, phosphodiesterase type 5 inhibitors, soluble guanylate cyclase stimulators, prostacyclin analogs, and prostacyclin IP receptor agonists have been developed for treating PAH and have shown to be effective in improving patient prognosis.[4] Thus, elucidation of the correlation between PPS and PAH pathogeneses may enable the application of PAH therapies to simultaneously treat PPS.

This study aimed to improve the prognosis of severe PPS by elucidating the genetic background of patients with severe PPS and the underlying mechanisms of pathogenesis. Additionally, the pathogeneses of PPS and PAH were comparatively analyzed.

METHODS

Data Availability

The data that support the findings of this study are available from the corresponding author upon reasonable request.

Study Population

We assessed the clinical profile of the first patient with PPS and Williams syndrome (WS) (Proband-1) and performed genetic testing and functional analyses of the disease-related gene candidate as described later in the article. Furthermore, to identify other patients with the candidate gene mutation, we performed genetic testing in an additional 12 patients with mild-to-severe PPS, 50 patients with WS without PPS, and 21 patients with severe PPS who did not have WS.

PPS Definition

In this study, severe PPS is defined as (1) a peak pressure gradient >50 mm Hg on cardiac catheterization or cardiac ultrasonography in at least 1 branch of the pulmonary artery[5] or (2) PPS with right systolic ventricular pressure elevated above 50 mm Hg on cardiac catheterization based on the recommendation of Cuypers et al.[6]

Genetic Analysis

Genomic DNA was extracted from peripheral blood lymphocytes or lymphoblastoid cells using the SepaGene DNA extraction kits (Sankyo Jyun-yaku, Tokyo, Japan), following the manufacturer's instructions.

Deletion of the chromosomal region 7q11.23 was confirmed using multiplex ligation-dependent probe amplification (SALSA MLPA Probemix P029 WBS, MRC-Holland, Amsterdam, Netherlands) with a 3130xl genetic analyzer (Thermo Fisher Scientific). The DNA sample of the patient was subjected to whole-exome sequencing (WES). A sequencing library was constructed using the SureSelect Human All Exon V6 kit (Agilent Technologies Inc., Santa Clara, CA, USA). Raw sequence data were generated using the Illumina NovaSeq6000 platform (Illumina, San Diego, CA, USA) with a standard 150-bp

paired-end read protocol at Macrogen Japan Corp (Tokyo, Japan). Sequencing data were processed on the Genome Reference Consortium Human Build 37 (GRCh37) assembly using the pipeline described earlier.[7] All procedures were performed according to the manufacturer's instructions.

The WES data were filtered using Clinvar (https://www.ncbi.nlm.nih.gov/clinvar/, updated November 5, 2022) and Genome Aggregation Database v3.1.2. (https://gnomad.broadinstitute.org/) to remove common polymorphisms, which was confirmed using direct sequencing with a 3130xl genetic analyzer (Thermo Fisher Scientific). The functional effects of the detected variants were evaluated using Combined Annotation Dependent Depletion version 1.6 (http://cadd.gs.washington.edu/). The functions of the candidate genes were determined using the Online Mendelian Inheritance in Man database (https://www.omim.org/) and published literature. As the parents of the 2 probands did not provide consent for DNA analysis, only the patients' DNA was analyzed.

In case of a suspected gross deletion/duplication in the WES, microarray-based comparative genomic hybridization analysis and droplet digital polymerase chain reaction (PCR) were performed.[8,9] In microarray-based comparative genomic hybridization analysis, the genomic copy numbers of the patients were determined using the GenetiSure Dx Postnatal Assay (Agilent Technologies, Santa Clara, CA, USA) according to the manufacturer's instructions. Droplet digital PCR was performed using a QX200 Droplet Digital PCR System and Quan-taSoft v1.7.4 (Bio-Rad Laboratories, Hercules, CA, USA). The droplet digital PCR primers targeting candidate genes were originally designed as described in Table S1.

Plasmid Construction

The human pCMV-HA-N-prostaglandin I_2 synthase (PTGIS) plasmid was constructed following the protocols of a previous study.[10] Each variant plasmid was constructed using a site-directed mutagenesis kit (Stratagene, CA, USA) according to the manufacturer's instructions. Human pulmonary artery endothelial cells (hPAECs) or human pulmonary artery smooth muscle cells (hPASMCs) were transfected with wild-type (WT) or variant pCMV-HA-N-PTGIS constructs using Lipofectamine 3000 reagent (Invitrogen, CA, USA). hPAECs and hPASMCs were harvested after an appropriate time and used for analysis.

pcDNA3.1(+)-3xFLAG-P2A-EGFP-PTGIS plasmids were used for immunofluorescence analysis to validate that transfection occurred successfully.

Cell Preparation and Culture

hPAECs (PromoCell, Heidelberg, Germany) were maintained in an endothelial cell growth medium (PromoCell). Cells that had been passaged 4 to 12 times were used for the experiments.

Distal hPASMCs were derived from small vessels (<2 mm in diameter) of lung resection specimens as described previously.[11] All hPASMCs were harvested from a site distant from the carcinoma. Table S2 shows the details of patients from whom the cells were derived. None of the patients exhibited pulmonary hypertension or underwent chemotherapy or radiation therapy. The lung parenchyma was dissected from a pulmonary arteriole, following the arteriolar tree, to isolate vessels with a diameter of 0.5 to 2 mm. The vessels were dissected, cut into small fragments, plated in T25 flasks, and allowed to adhere for 2 hours. The cells were cultured in Dulbecco's modified Eagle medium/high-glucose (Sigma, St. Louis, MO, USA) supplemented with 10% fetal bovine serum (Gibco, New York, NY, USA) and 100 U/mL penicillin–streptomycin (Gibco) at 37 °C in a humidified 5% CO_2 incubator. For analysis, cells that had been passaged 5 to 9 times were used.

Based on the findings reported by Pak et al., we additionally conducted cell culture under hypoxic conditions.[12] For hypoxia treatment, transfected hPAECs and hPASMCs were maintained in 10% O_2 using a BIONIX hypoxic culture kit (Sugiyama-Gen, Tokyo, Japan) according to the manufacturer's instructions.

Cell Analysis

Quantitative Real-Time-PCR

Total cellular RNA was extracted from 2.0×10^5 cells using an RNeasy Mini Kit (QIAGEN, Hilden, Germany) according to the manufacturer's instructions. For PCR analysis, 1 μg of RNA was reverse-transcribed to cDNA using Superscript III reverse transcriptase and random hexamer primers (Invitrogen). Real-time PCR analysis was performed on a Thermo Fisher Scientific applied Biosystems QuantStudio 5 system (Applied Biosystems, Foster City, CA, USA) using SYBR Green PCR Master Mix (Applied Biosystems). The reaction consisted of 10 μL of SYBR Green PCR Master Mix, 1 μL of a 5 mmol/L mix of forward and reverse primers, 8 μL of water, and 1 μL of template cDNA for a total volume of 20 μL. Cycling was performed using a QuantStudioTM5 RealTime PCR thermal cycler (Applied Biosystems). The relative expression of each gene was normalized against that of 18S rRNA. The data are presented as the mean±SD. The primers used for quantitative real-time PCR analysis are shown in Table S3.

Western Blotting

Western blotting analysis was performed with confluent human embryonic kidney 293T cells (RIKEN Cell Bank), which were lysed using radioimmunoprecipitation assay

buffer containing protease inhibitors (Nacalai Tesque, Kyoto, Japan). The cell lysates were boiled in sodium dodecyl sulfate loading buffer and resolved using sodium dodecyl sulfate-polyacrylamide gel electrophoresis with a 12% gel. The resolved proteins were transferred to a polyvinylidene fluoride membrane using the semi-dry blotting method. The membrane was blocked with 5% BSA and incubated with anti-PTGIS (ab23668, Abcam, Cambridge, UK, 1000×) or anti-ACTB antibodies (Sigma, 10000×) in 5% BSA overnight. Next, the membrane was incubated with horseradish peroxidase-conjugated goat antirabbit IgG (Kirkegaard & Perry Laboratories, Gaithersburg, MD, USA) or antimouse IgG (Kirkegaard & Perry Laboratories) to detect PTGIS or ACTB, respectively. Immunoreactive signals were developed using enhanced chemiluminescence and ImageQuant LAS 4000 (GE Healthcare, Chicago, IL, USA).

Cell Viability Assay

The viability of hPAECs or hPASMCs was determined using a cell proliferation assay with the WST-8 reagent (Dojindo, Kumamoto, Japan). This assay is based on the detection of formazan, generated through the cellular mitochondrial dehydrogenase-mediated cleavage of the tetrazolium salt WST-8.

Caspase 3/7 and Prostacyclin Detection

Transfected hPAECs or hPASMCs were stimulated with 10 ng/mL tumor necrosis factor-α and 20 μg/mL cycloheximide for 3 hours to induce apoptosis. The activity of caspase 3/7 was determined using the Caspase-Glo® 3/7 Assay System (Promega, WI, USA), following the manufacturer's instructions.

As prostacyclin has a short half-life, the amount of prostacyclin in the culture supernatant of hPAECs or hPASMCs was monitored by measuring the level of its stable metabolite, 6-keto-prostaglandin f1alpha ($PGF_{1\alpha}$), using an enzyme-linked immunosorbent assay kit (Cayman Chemical Company, Ann Arbor, MI, USA).

Tube Formation and Migration Assay

Endothelial tube formation was assessed using the μ-slide 3D Well angiogenesis assay (ibidi, Germany). In brief, 10 μL of Matrigel (BD Biosciences) was spread on the bottom of a μ-slide 3D well and incubated at 37 °C until the gel solidified. Subsequently, 50 μL of suspension containing 1×10^4 treated hPAECs was cultured on Matrigel. Photographs were captured under a phase-contrast microscope (Leica, Wetzlar, Germany) at 4 hours.

The migration ability of hPAECs was assessed using the wound-healing assay. Briefly, 2×10^4 treated cells were seeded per well containing Culture-Inserts (ibidi) overnight; the inserts were removed the next day, and the culture medium was replaced with serum-free medium. Photographs were captured under a phase-contrast microscope (Leica) at 0, 4, 8, and 24 hours.

Immunostaining of Lung Tissue From Proband-1

Proband-1 with severe PPS underwent an emergency right middle lobectomy owing to a ruptured pulmonary artery pseudoaneurysm at 12 years of age. The lung tissue specimens were subjected to immunostaining. As most of the lung specimens available in our hospital were collected from adult patients with primary or metastatic lung cancer, these individuals constituted a considerable proportion of the control group. Table S4 shows the details of the patients from whom the lung tissue was collected. As nicotine inhibits prostacyclin production,[13] we selected only nonsmokers as controls. The normal section of lung tissue from patients who had undergone pneumonectomy for other diseases was used. In the cancer control group, lung tissue sufficiently distant from lung cancer tissue and pathologically confirmed to be free of cancer cells was used. Written informed consent was obtained from all patients or their guardians.

Each paraffin-embedded lung tissue was sliced into 3 to 4-μm-thick sections. To perform hematoxylin and eosin staining, the paraffin-embedded lung tissue sections were dewaxed with xylene solution, dehydrated with an alcohol gradient, and washed with water. The sections were then stained with hematoxylin for 5 minutes. After the excess dye was washed off, the sections were acidified with hydrochloric acid and ethanol and stained with eosin for 5 minutes. The excess dye was washed off, and the sections were dehydrated using an ethanol gradient and dried. The deparaffinized and rehydrated lung tissues were subjected to immunostaining.

Antigen retrieval was performed using an EnVision FLEX Target retrieval solution (Dako, Agilent Technologies, CA, USA), following the manufacturer's protocol. The sections were incubated with DAKO Envision ex peroxidase blocking reagent for 5 minutes to block endogenous peroxidase. Next, the sections were incubated with anti-PTGIS antibodies (ab23668, Abcam, UK, 800×) for 30 minutes.

To perform immunofluorescence staining, the deparaffinized and rehydrated sections were processed for antigen retrieval using a standard microwave heating technique. The sections were incubated in phosphate-buffered saline with 10% goat serum for 1 hours at 25 °C followed by incubation with rabbit polyclonal anti-PTGIS (ab23668, Abcam, UK, 800×) or mouse monoclonal antihuman CD31 antibodies (clone JC70A, DAKO, 50×) for 1 hour at 25 °C. Next, the sections were labeled with Alexa 594-conjugated goat antirabbit IgG or Alexa 488-conjugated goat antimouse IgG (Invitrogen, Tokyo, Japan) antibodies and observed under a fluorescence

microscope. The fluorescence signals of PTGIS and CD31 were analyzed using the ImageJ software (version 1.53e; National Institutes of Health, Bethesda, MD, USA; https://imagej.nih.gov/ij). The control group comprised tissues from the 6 cases listed in Table S4. The data are expressed as the PTGIS/CD31 ratio.

Urine Analysis of Proband-1

Urine samples were collected from Proband-1 and 10 healthy male control individuals and stored at −80 °C. Written informed consent was obtained from all participants. To avoid the admixture of kidney-derived 6-keto $PGF_{1\alpha}$ and to measure plasma-derived prostacyclin in urine samples, prostaglandin I metabolite was used as an indicator.[14] The urinary levels of prostaglandin I metabolite were measured using enzyme-linked immunosorbent assay (Cayman Chemical Company). The levels of urinary metabolites were normalized to those of urinary creatinine, which was measured at a central laboratory (SRL Co., Tokyo, Japan) using the enzymatic creatinine assay method.

Statistical Analysis

Data are presented as the mean±SD. The results of cell viability, quantitative real-time PCR analysis, apoptosis assay, 6-keto-$PGF_{1\alpha}$ analysis, prostaglandin I metabolite analysis, and immunostaining were evaluated using 1-way ANOVA, followed by Dunnett's test. Univariate comparisons between groups were performed using unpaired *t* tests for continuous variables. Differences were considered significant at $P<0.05$. All statistical analyses were performed using JMP Pro 16 (SAS Institute, Cary, NC, USA).

Ethics Approval

This study was approved by the Institutional Review Board of the Hokkaido University Hospital (Institutional Review Board approval Nos.: 020–0212 and 022–0178) and Peking Union Medical College (Institutional Review Board approval No.: JS-2880). Written informed consent was obtained from the guardians of patients with PPS or PAH according to the regulations of the Declaration of Helsinki.

Experiments on human lung tissues were approved by the Institutional Review Board of the Hokkaido University Hospital for clinical research (Institutional Review Board approval Nos.: 019-0432 and 020-0212). Informed consent was obtained from all individuals.

Case Presentation of Proband-1

The male patient was delivered without asphyxia at a gestational age of 37 weeks with a body weight of 2410 g. After birth, the patient had a heart murmur and was diagnosed with a small secundum atrial septal defect using cardiac ultrasonography. During outpatient follow-up, the patient was suspected of having WS as they exhibited typical elfin-like facial features, inguinal hernia, congenital heart disease, and stunted growth. Fluorescence in situ hybridization analysis revealed a microdeletion in the 7q11.23 region, which confirmed WS (data not shown). PPS became apparent and gradually worsened. The patient underwent a cardiac catheterization test at the age of 7 years. Multiple peripheral stenoses (Gay type 3) were detected, which caused the systolic right ventricular pressure to exceed the systolic left ventricular pressure (105 and 95 mm Hg, respectively). The peak pressure gradient from the distal right pulmonary artery to the proximal right pulmonary artery was 50 mm Hg, and the peak pressure gradient from the distal left pulmonary artery to the proximal left pulmonary artery was 45 mm Hg. Percutaneous transluminal pulmonary angioplasty was not performed because the operative risk was high.

Most PPS cases in patients with WS can resolve spontaneously. Hence, the patient was followed up without treatment. At the age of 12 years, mechanical ventilation was required owing to pneumonia and bloody sputum. The patient was diagnosed with a pseudoaneurysm of the middle lobe branch of the right pulmonary artery and underwent a right middle lobectomy. At the age of 15 years, the percutaneous oxygen saturation of the patient decreased to 90%. Home oxygen therapy was initiated at the age of 16 years. However, the percutaneous oxygen saturation level remained low (below 80%) and decreased to 60% when the patient developed a respiratory infection.

At the age of 17 years, the patient was admitted to our department for a second cardiac catheterization. The clinical characteristics of the patient at the time of admission were as follows: height, 154 cm; weight, 60.4 kg; heart rate, 96 bpm; blood pressure, 121/78 mm Hg; percutaneous oxygen saturation, 92% (receiving supplemental oxygen via nasal cannula at 3 L/min). Physical examination revealed a grade 3/6 systolic heart murmur. Chest radiography revealed enhanced pulmonary vascular shadows and right ventricular hypertrophy. Electrocardiography revealed a strain pattern in leads V1 through V3, suggesting right ventricular pressure overload.

During cardiac catheterization, pulmonary arteriography revealed diffuse stenosis of the pulmonary artery with a thin peripheral side. The diameters of the narrowest portion of the left and right pulmonary arteries were 0.9 and 1.2 mm, respectively. Additionally, an aneurysm was observed in the left pulmonary artery, a site on the peripheral side of the stenotic region (Figure 1A). Chest contrast computed tomography showed flattening of the ventricular septum due to increased right ventricular pressure (Figure 1B). Pulmonary blood flow scintigraphy showed a heterogeneous blood flow deficit (Figure 1C). Catheterization also revealed elevated pulmonary arterial pressure (105/38 mm Hg, mean 66 mm Hg) with a cardiac index

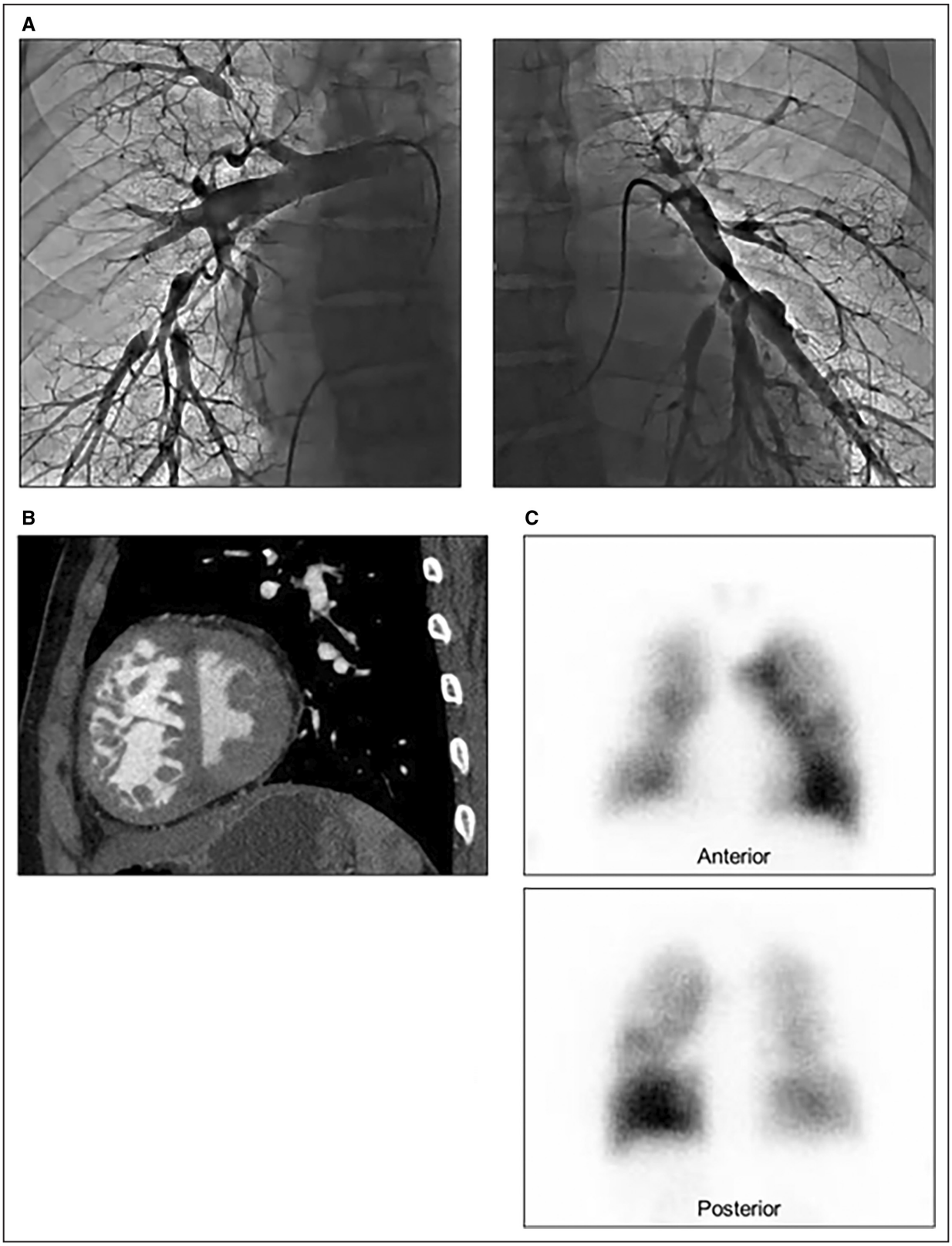

Figure 1. Imaging findings of Proband-1 with severe peripheral pulmonary stenosis.
A, Pulmonary angiography reveals diffuse, peripheral pulmonary artery stenosis and pulmonary artery aneurysm formation. The right middle lobe of the lung was resected at the age of 12 years. **B**, Chest contrast computed tomography shows flattening of the ventricular septum due to increased right ventricular pressure. **C**, Pulmonary blood flow scintigraphy shows a heterogeneous blood flow defect.

of 2.0 L/min·m^2. Systolic right and left ventricular pressures were 103 and 120 mm Hg, respectively.

We first considered whether percutaneous transluminal pulmonary angioplasty was feasible for this condition. However, we were concerned about new aneurysms developing and the risk of bleeding owing to the sudden high pressure on the peripheral side after percutaneous transluminal pulmonary angioplasty. Moreover, surgical treatment was expected to cause extensive damage to a large portion of the lung parenchyma by the time multiple peripheral stenoses occurred. Thus, an aggressive therapeutic intervention was considered challenging. Accordingly, the individual was monitored as an outpatient with continuous home oxygen therapy only. The indications for lung transplantation were also considered. However, the parents did not wish to consider this option.

RESULTS

Multiplex ligation-dependent probe amplification revealed a heterozygous deletion in the region associated with WS (Figure S1). Furthermore, WES-based copy number analysis revealed a deletion of chromosome 7q11.23—typical for WS (Figure S2). Therefore, the possibility of another disease-causing genetic abnormality was examined to detect other factors contributing to severe PPS.

WES did not reveal other pathological variants, such as *RNF213* or *JAG1*, which are involved in the onset of PPS.[15,16] However, a *PTGIS* nonsense variant (NM_000961: c.940 G>T p. Glu314Ter [p.E314X], rs13306027) was identified in Proband-1 (Figure S3). The p.E314X variant was located between the transmembrane domain and the heme-binding site (Figure S4).[17] The Combined Annotation Dependent Depletion score was 33. In the Genome Aggregation Database, the allele frequencies of the variant among all ethnicities and East Asian individuals were 0.0000394 and 0.0001927, respectively (Table 1).

PTGIS WT, 2 previously reported pathological *PTGIS* variants in patients with PAH (c.755G>A p.Arg252Glu[p.R252Q] (rs759344518) and c.1339G>A p.Ala447Thr [p.A447T] (rs146531327)),[10] and the *PTGIS* p.E314X variant were overexpressed in human embryonic kidney 293T cells, hPASMCs, and hPAECs.

Quantitative real-time PCR analysis revealed that transfection with the *PTGIS* p.E314X variant construct downregulated *PTGIS* mRNA expression in hPAECs and hPASMCs (Figure S5). Furthermore, western blotting revealed that the expression of PTGIS in the *PTGIS* p.E314X construct-transfected cells was not significantly different from that in the empty construct-transfected cells (Figure S6). The successful transfection of control *PTGIS* and *PTGIS* p.E314X plasmids into hPAECs and hPASMCs was confirmed via immunostaining (Figure S7). Moreover, the viability of hPAECs transfected with the *PTGIS* variant constructs was significantly higher than that of hPAECs transfected with the WT *PTGIS* construct (Figure 2A and 2B). However, transfection with the *PTGIS* WT, p.A447T, and p.E314X constructs did not significantly affect hPASMC viability (Figure 2C and 2D).

The effect of each variant on apoptosis was assessed by examining caspase 3/7 activity after stimulation with tumor necrosis factor-α and cycloheximide (Figure 3A through 3D). Caspase 3/7 activity in *PTGIS* p.E314X construct-transfected hPAECs was significantly lower than that in *PTGIS* WT construct-transfected hPAECs. Furthermore, caspase 3/7 activity in *PTGIS* p.E314X construct-transfected hPASMCs was significantly lower than that in *PTGIS* WT construct-transfected hPASMCs under hypoxic conditions.

Table 1. Characteristics of 2 Patients With Severe PPS and *PTGIS* Rare Variants

Proband no.	Nucleotide change	1000 genomes	EVS	gnomAD all ethnicities	gnomAD East Asian	CADD score	Clinvar	Cardiac catheterization data	Outcome
1	p.E314X	None	None	0.000039	0.000193	33	Not available	Systolic right ventricular pressure 105 mm Hg, systolic left ventricular pressure 95 mm Hg, peak pressure gradient from distal right pulmonary artery to proximal right pulmonary artery 50 mm Hg, peak pressure gradient from distal left pulmonary artery to proximal left pulmonary artery 45 mm Hg	Survived
2	c.1358+2T>C	None	None	0.000395	0.001	32	Pathogenic	Peak pressure gradient from distal left pulmonary artery to proximal left pulmonary artery 88 mm Hg, main pulmonary artery 117/29 (70) mm Hg	Died

Values other than the CADD score indicate allele frequencies. CADD indicates Combined Annotation Dependent Depletion; EVS, Exome Variant Server; gnomAD, Genome Aggregation Database; and PPS, peripheral pulmonary stenosis.

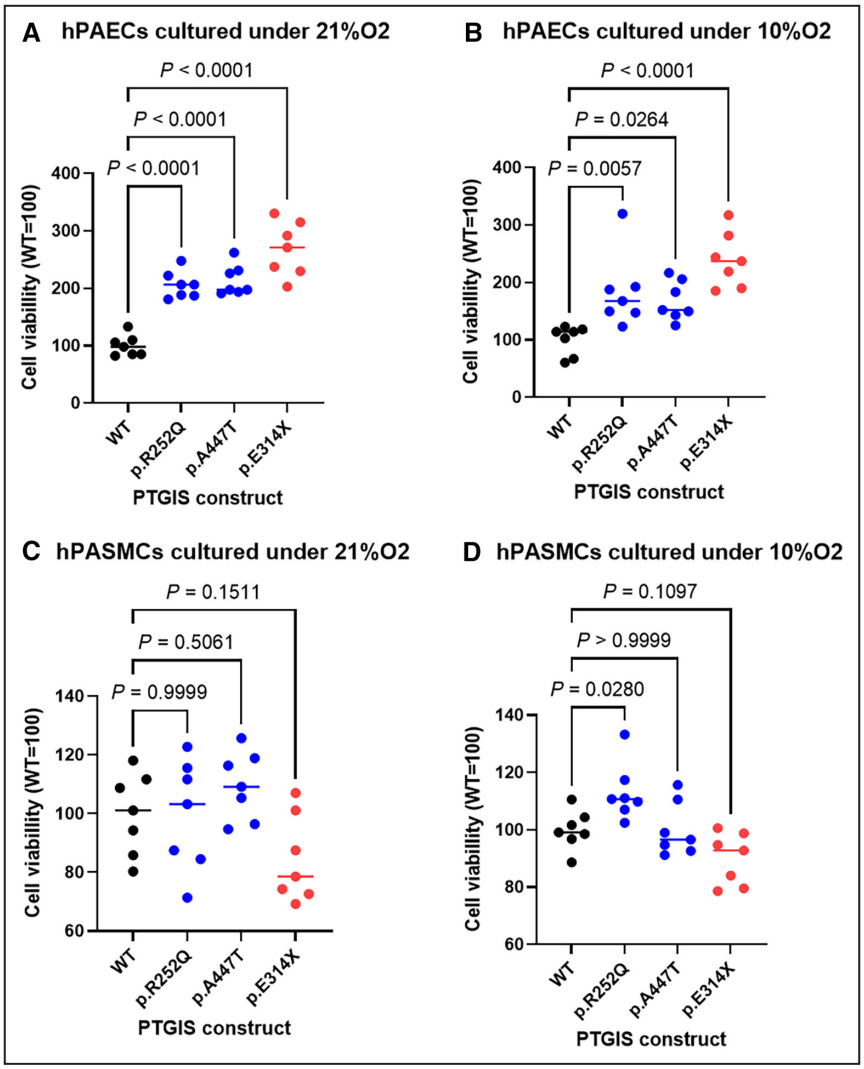

Figure 2. Overexpression of *PTGIS* variants increases the viability of hPAECs. Viability of hPAECs cultured under normoxic (21% oxygen) (**A**, n=7 per group) or hypoxic (10% oxygen) (**B**, n=7 per group) conditions analyzed on day 3 post transfection with the *PTGIS* WT or variant constructs. Viability of hPASMCs cultured under normoxic (**C**, n=7 per group) or hypoxic (**D**, n=7 per group) conditions analyzed on day 2 post transfection with the *PTGIS* WT or variant constructs. The values represent the mean±SD from independent experiments. Groups were compared using 1-way ANOVA followed by Dunnett's test (control=WT). The mean values are represented as a percentage relative to those in the hPAECs or hPASMCs transfected with the *PTGIS* WT construct. hPAECs indicates human pulmonary artery endothelial cells; hPASMCs, human pulmonary artery smooth muscle cells; PTGIS, prostaglandin I_2 synthase; and WT, wild-type.

Next, the amount of 6-keto-$PGF_{1\alpha}$ in transfected cells was comparatively analyzed. Under hypoxic conditions, the production of 6-keto-$PGF_{1\alpha}$ in hPAECs transfected with the *PTGIS* variant constructs was significantly downregulated when compared with that in hPAECs transfected with the *PTGIS* WT construct (Figure 4A and 4B). In contrast, the production of 6-keto-$PGF_{1\alpha}$ did not differ significantly between *PTGIS* WT construct-transfected and *PTGIS* variant construct-transfected hPASMCs (Figure 4C and 4D).

Furthermore, we performed a tube formation and migration assay using hPAECs. hPAECs treated with the *PTGIS* p.E314X plasmid were less likely to form branching vessels, and the branching vessels were shorter than those of cells treated with the control plasmid (Figure 5A through 5C). The migration assay revealed that after 8 and 24 hours, hPAECs treated with the *PTGIS* p.E314X plasmid exhibited higher migration ability than those treated with the control plasmid (Figure 5D and 5E). The tube formation and migration assays conducted using

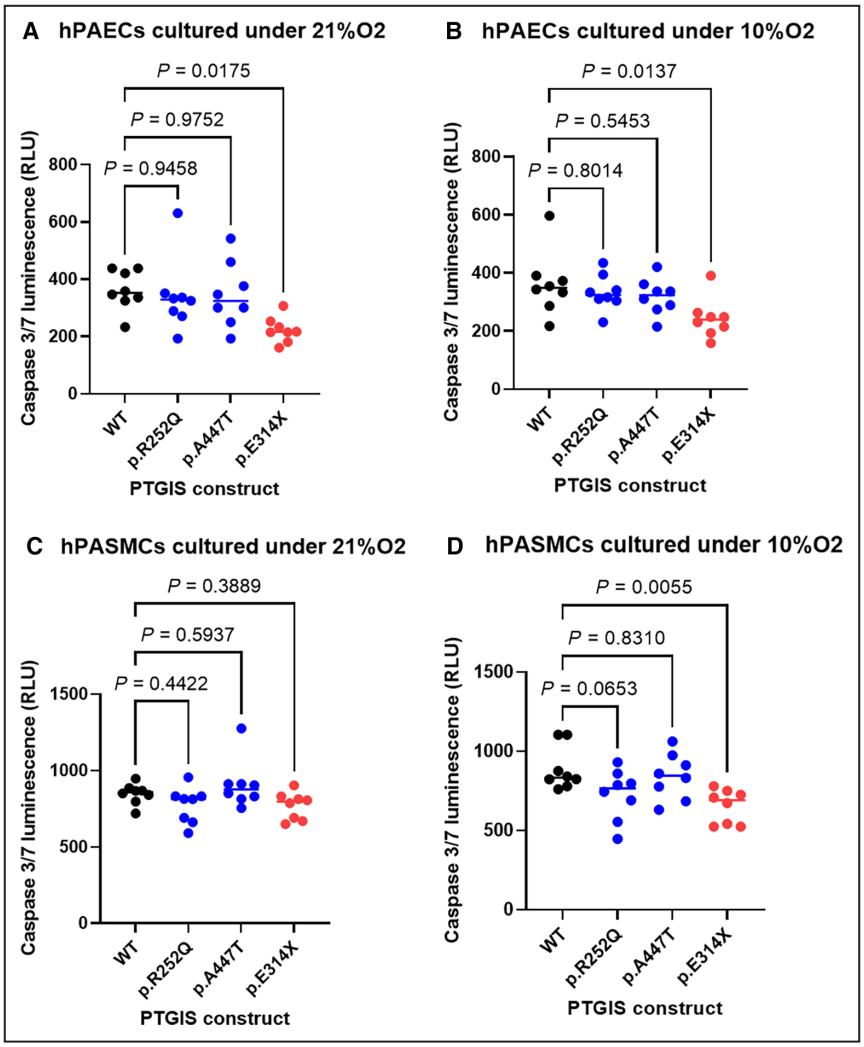

Figure 3. *PTGIS* p.E314X overexpression downregulates caspase 3/7 under varying oxygen conditions.
Viability of hPAECs cultured under normoxic (**A**, n=8 per group) or hypoxic (**B**, n=8 per group) conditions analyzed on day 1 post transfection with *PTGIS* WT or variant constructs. Viability of hPASMCs cultured under normoxic (**C**, n=8 per group) or hypoxic (**D**, n=8 per group) conditions analyzed on day 1 post transfection with *PTGIS* WT or variant constructs. The values represent the mean±SD from independent experiments. Groups were compared using 1-way ANOVA followed by Dunnett's test (control=WT). Mean values are represented as percentages relative to those in hPAECs or hPASMCs transfected with the WT *PTGIS* construct. hPAECs indicates human pulmonary artery endothelial cells; hPASMCs, human pulmonary artery smooth muscle cells; PTGIS, prostaglandin I_2 synthase; RLU, relative luminescence unit; and WT, wild-type.

PTGIS p.A447T and *PTGIS* p.R252Q plasmids yielded nearly identical results (Figure S8).

Finally, the pathological changes in the pulmonary arteries and urine of Proband-1 were analyzed. Hematoxylin and eosin staining revealed irregular thickening of the intima and edematous thickening between the intima and media in Proband-1 with PPS. These changes were accompanied by pulmonary arterial stenosis (Figure 6A). Immunostaining of pulmonary arteries with the anti-PTGIS antibodies revealed that PTGIS was primarily expressed in the pulmonary artery endothelium (Figure 6B). Double-color immunofluorescence staining with the anti-CD31 (endothelial cells) and anti-PTGIS antibodies confirmed that PTGIS expression in the pulmonary artery endothelium of Proband-1 with PPS was significantly lower than that in the pulmonary artery endothelium of the control individuals (Figure 6C through 6D). The urinary levels of prostaglandin I metabolites were also compared between Proband-1 with PPS and healthy controls. The levels of urinary prostaglandin I metabolites, which were normalized to the urinary creatinine levels, were

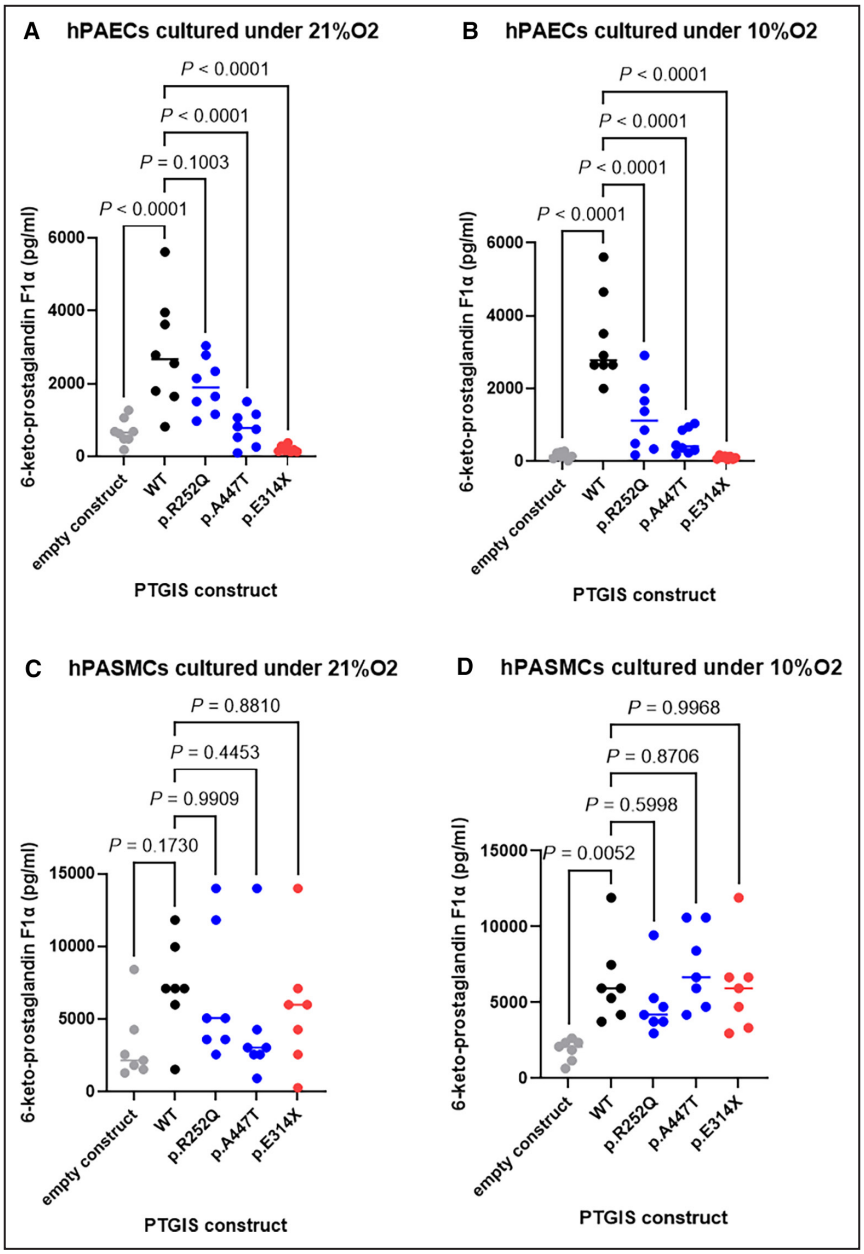

Figure 4. *PTGIS* variants downregulate 6-keto-PGF1α in hPAECs under hypoxic conditions.

Concentration of 6-keto-$PGF_{1\alpha}$ in the culture supernatant of hPAECs cultured under normoxic (21% oxygen) (**A**, n=8 per group) or hypoxic (10% oxygen) (**B**, n=8 per group) conditions. Concentration of 6-keto-$PGF_{1\alpha}$ in the culture supernatant of hPASMCs cultured under normoxic (21% oxygen) (**C**, n=8 per group) or hypoxic (10% oxygen) (**D**, n=8 per group) conditions. The values represent the mean±SD from independent experiments. Groups were compared using 1-way ANOVA followed by Dunnett's test (control=WT). hPAECs indicates human pulmonary artery endothelial cells; hPASMCs, human pulmonary artery smooth muscle cells; PTGIS, prostaglandin I_2 synthase; WT, wild-type; and 6-keto-$PGF_{1\alpha}$, 6-keto-prostaglandin f1alpha.

significantly downregulated in Proband-1 with PPS compared with those in the controls (Figure 6E).

Furthermore, a heterozygous splice-site variant, c.1358+2 T>C, rs13306026, was identified in 1 patient with WS and severe PPS (Proband-2). In Clinvar, the c.1358+2 T>C variant is described as a pathogenic variant in essential hypertension, which causes skipping of exon 9 of *PTGIS*.[18] Proband-2 had multiple PPS; a cardiac catheterization performed at the age of 12 years revealed a high-pressure gradient from the

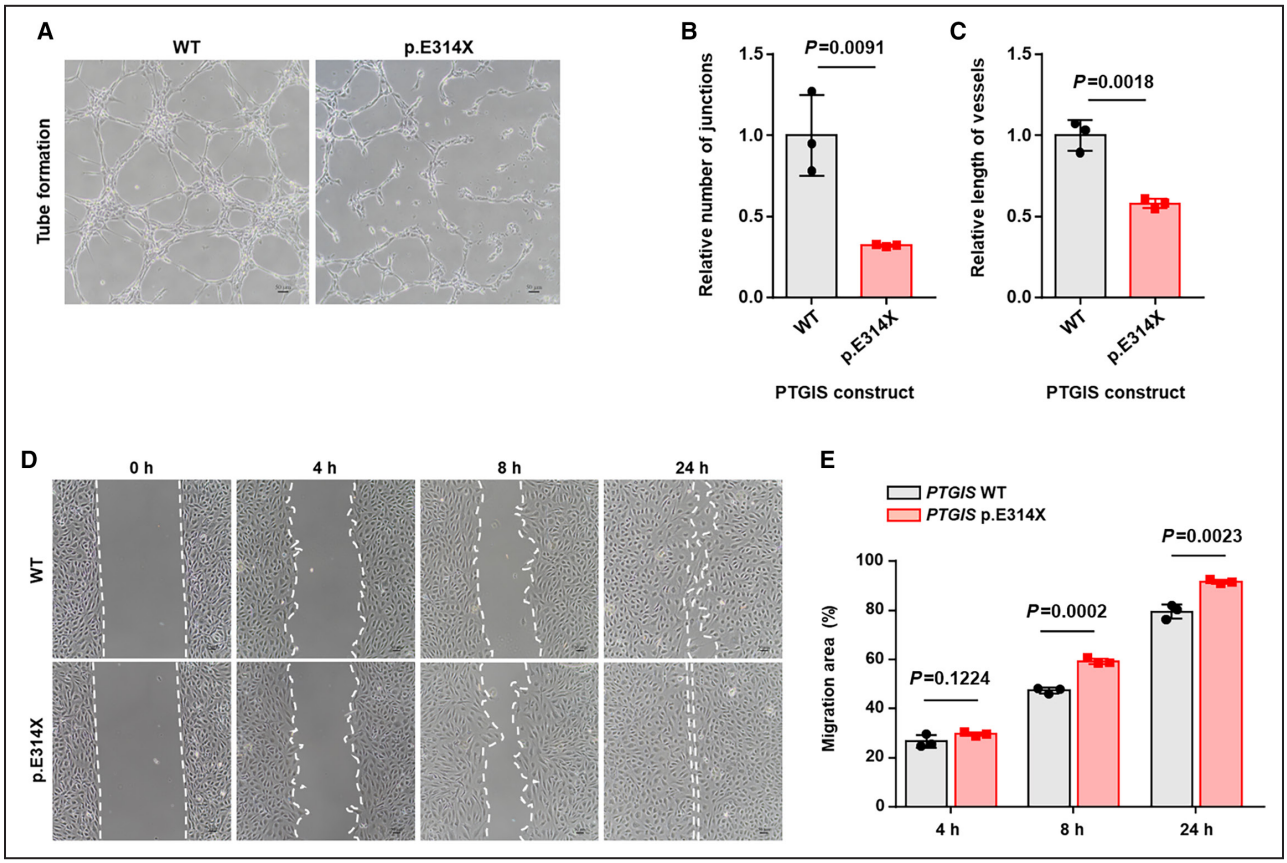

Figure 5. Characteristics of hPAECs treated with *PTGIS* p.E314X or control plasmid.
A, Angiogenetic ability of hPAECs treated with Control or *PTGIS* p.E314X plasmid. Scale bars: 50 μm. Number of junctions (**B**, n=3 per group) and length of vessels (**C**, n=3 per group) per field analyzed using ImageJ software. The data are presented as the mean±SD. $^{**}P<0.01$ (**D**) Migration ability of hPAECs treated with Control or *PTGIS* p.E314X plasmid, as determined with a wound-healing assay. Images captured at 0, 4, 8, and 24 hours. Scale bars: 50 μm. (**E**, n=3 per group) Percentage of migration area quantified by ImageJ. The data are presented as the mean±SD. Groups were compared using an unpaired *t* test with a 95% CI. hPAECs indicates human pulmonary artery endothelial cells; and PTGIS, prostaglandin I_2 synthase.

distal to proximal left pulmonary artery (88 mm Hg) and high main pulmonary artery pressure (systolic pressure was 117 mm Hg, diastolic pressure was 29 mm Hg, and mean pressure was 70 mm Hg); the PPS was deemed to be severe. The patient suffered cardiopulmonary arrest because of severe PPS at age 15 years and subsequently died of bacterial infection. Genetic testing in the family was not possible following the patient's death (Table 1).

DISCUSSION

This study identified 2 rare variants of *PTGIS*, a candidate disease-causing gene, in 2 patients with WS with severe PPS. The findings of this study demonstrate that the p.E314X variant suppresses PTGIS expression and cell proliferation in hPAECs and causes pulmonary arterial stenosis. The presence of *PTGIS*-p.E314X leads to impaired formation of normal blood vessels by PAECs, and increased PAEC migration may contribute to abnormal proliferation in the pulmonary arterial intima. This supports the pathological observations noted in Proband-1. Hence, this is the first report of a genetic association between WS and *PTGIS*.

PTGIS is located on chromosome 20q13.13. According to the Human Protein Atlas version 20.1 (https://www.proteinatlas.org/), PTGIS is expressed in several organs, including the lungs, and cells, including smooth muscles. Moreover, single-cell analysis revealed that PTGIS expression is upregulated in fibroblasts and endothelial cells. An immunohistochemical study reported the expression of PTGIS in vascular endothelial and smooth muscle cells.[19] This expression pattern is consistent with the findings of the current study.

PTGIS, a member of family 8 of the cytochrome P450 superfamily,[20] catalyzes the conversion of prostaglandin H_2 to prostaglandin I_2. Prostaglandin I_2, also known as prostacyclin, is a potent vasodilator and inhibitor of platelet aggregation.[21] Moreover, several studies have reported an association between PTGIS and

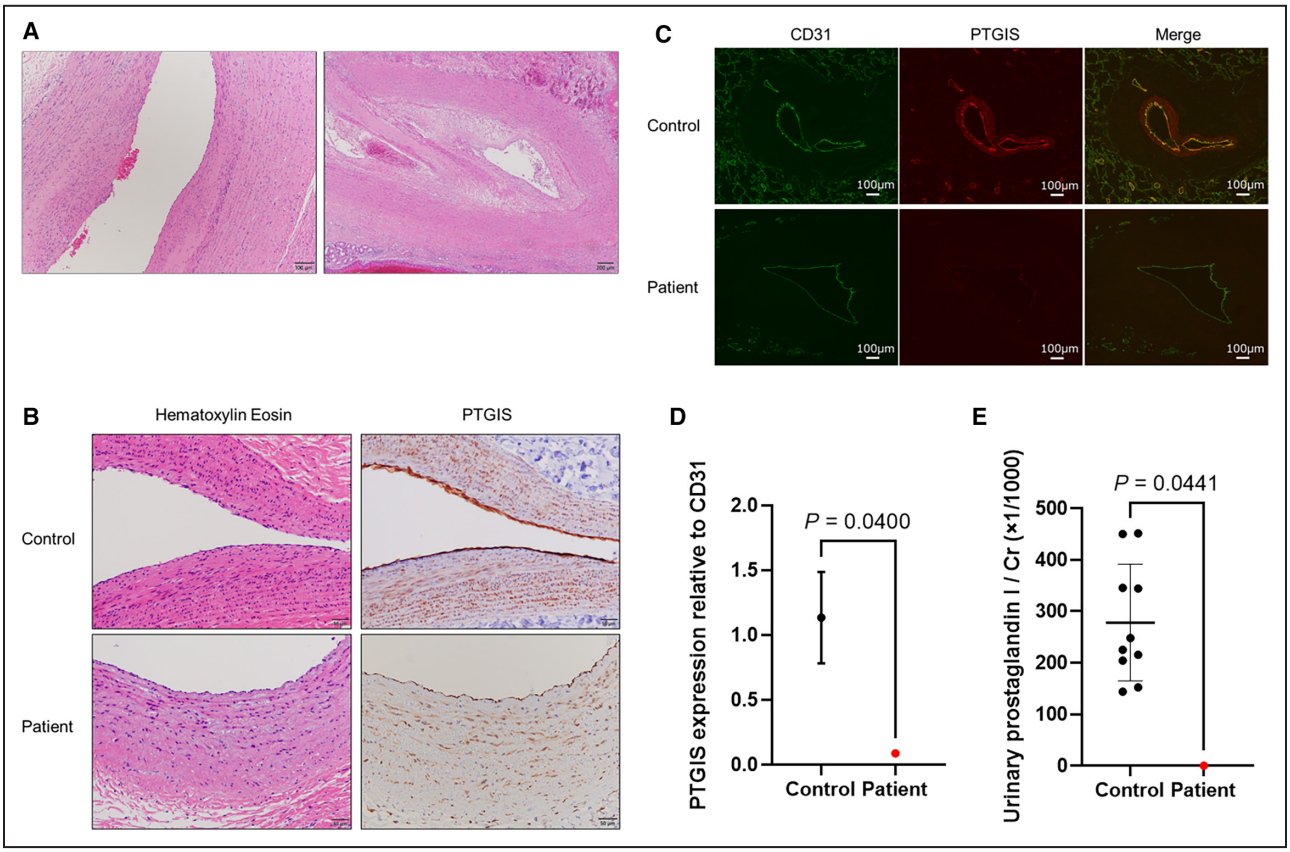

Figure 6. Pulmonary artery endothelial PTGIS levels and urinary prostaglandin I metabolites in Proband-1 and healthy controls.

A, Hematoxylin and eosin staining of pulmonary artery sections of Proband-1; irregular thickening of the intima and edematous thickening is present between the intima and media. **B**, Immunostaining analysis: PTGIS is expressed mainly in the pulmonary artery endothelium. **C** and **D**, CD31 immunostaining (green) signal localized to the pulmonary artery endothelium. PTGIS expression (red) is distinct in the healthy controls and downregulated in Proband-1 with PPS. PTGIS density is normalized to CD31 density. The values of the control group (n=6) represent the mean±SD. Groups were compared using an unpaired *t* test (**P*<0.05). **E**, The levels of urinary prostaglandin I metabolites were significantly downregulated in Proband-1 with PPS compared with those in the controls. The values of the control group (n=10) represent the mean±SD from healthy controls. The levels of urinary prostaglandin I metabolites were normalized to those of urinary creatinine. For each participant, the measurement was carried out three times. Groups were compared using an unpaired *t* test with a 95% CI. PPS indicates peripheral pulmonary stenosis; and PTGIS, prostaglandin I_2 synthase.

different cancers, liver fibrosis, and endometriosis. For example, downregulation of PTGIS expression reduces prostaglandin I_2 levels and is associated with aggressive tumor phenotypes and poor disease prognosis. Similarly, kidney renal papillary cell carcinoma, lung adenocarcinoma, thyroid carcinoma, and uterine corpus endometrial carcinoma exhibit reduced PTGIS expression.[22,23] Zhuang et al. implicated 9 metabolism-related genes, including *PTGIS*, in the prognosis of squamous cell carcinoma of the lung.[24] Additionally, increased *PTGIS* expression inhibits the activation of hepatic stellate cells and reduces liver fibrosis.[25] Furthermore, PTGIS protein expression is increased in endometriosis lesions compared with that in normal uterine tissue, whereas its depletion in animal models of endometriosis can be therapeutic.[26,27] Thus, PTGIS has been linked to various diseases associated with cell proliferation.

Nakayama et al. identified *PTGIS* as a candidate gene for essential hypertension. They reported that a splice-site variant of *PTGIS*, generated through exon 9 skipping, encoded a truncated protein in 1 patient with essential hypertension. The siblings of the proband had the same splicing variant and exhibited hypertension.[18] Moreover, in 2020, Jing et al. identified 3 rare *PTGIS* loss-of-function variants (c.521+1G>A, p.R252Q, and p.A447T) in patients with idiopathic PAH.[9] The current study identified a nonsense variant of *PTGIS* in a pediatric patient with PPS. This finding suggests that PPS and PAH may share similar pathogenesis mechanisms and origins. The Genome Aggregation Database analysis results indicated that the pathogenic variants of *PTGIS* were rare and were detected marginally more frequently in East Asian individuals than in other racial groups.

Jing et al. also reported that treatment with iloprost, a prostaglandin I_2-replenishing drug, significantly decreased pulmonary vascular resistance in patients with PAH harboring the *PTGIS* variants p.R252Q and p.A447T.[9] Therefore, patients with PPS carrying *PTGIS* pathogenic variants may also benefit from treatment with PTGIS-replenishing drugs. Hence, drugs used to treat PAH can be repurposed to treat PPS. However, drug repositioning should be implemented with care as PTGIS-replenishing drugs may aggravate pulmonary artery pseudoaneurysms in cases similar to our Proband-1.

Jing et al. also analyzed the culture supernatant of pulmonary microvascular endothelial cells and reported that the antiapoptotic effects of the *PTGIS* variants p.R252Q and p.A447T were diminished compared with those of *PTGIS* WT variants.[9] p.R252Q and p.A447T are involved in the remodeling of small pulmonary arteries.[9] In the current study, caspase 3/7 activity in hPAECs and hPASMCs transfected with the *PTGIS* p.E314X construct was significantly lower than that in hPAECs and hPASMCs transfected with the *PTGIS* WT construct. However, caspase 3/7 activity in the *PTGIS* WT construct-transfected cells was similar to that in cells transfected with the *PTGIS* p.R252Q and p.A447T variant constructs. Moreover, we found that the p.E314X variant may act on the central pulmonary artery. However, there have been no reports of WS being associated with PAH. Hence, differences in the location of the variant may influence the phenotypic differences and the pathogenesis of PPS and PAH.

This study has several limitations. First, the contribution of WS to the severity of PPS is unknown. Most PPS in WS is mild with most cases found to resolve spontaneously.[27] However, in our patients with identified rare *PTGIS* variants, severe PPS did not improve but rather worsened. Based on the results of this study, the severity of PPS in these 2 patients with WS cannot be solely explained by WS. No other patients with WS in our study who lacked *PTGIS* pathogenic variants exhibited severe PPS. Thus, further studies are required to clarify the roles of the WS-associated 7q11.23 deletion and *PTGIS* rare variants, as well as the individual contribution of *PTGIS* rare variants, in the development of severe PPS. In addition, we detected rare *PTGIS* variants in only 2 patients with PPS. Hence, further research is required to ascertain whether other patients with PPS have these rare *PTGIS* variants. Second, PPS might be as severe in PPS patients with *RNF213* or *JAG1* pathogenic variants as in the 2 cases presented here.[14,15] Although the relationship between the *PTGIS* and these 2 genes could not be established in the present study, we recommend investigating PPS patients with *RNF213* or *JAG1* mutations for the coexistence of *PTGIS* pathogenic variants. Third, genetic analyses could not be performed on the family members of the patients because of the lack of consent. Furthermore, it is imperative to investigate the impact of pathogenic PTGIS variants on both hPAECs and hPASMCs under c-culture conditions in future studies. Finally, we were unable to detect *PTGIS* variants in PPS cases without WS. Hence, research on *PTGIS* variants and functional analysis in patients with PPS without WS are required to further elucidate the underlying pathology.

We recognize the uncertainty regarding the observed differences under normal and hypoxic conditions in Figures 2 and 3. However, as pulmonary arteries are naturally exposed to low oxygen conditions, culturing cells under hypoxic conditions is considered to be more physiologically relevant. This choice may account for the observed variations in results.

CONCLUSIONS

In conclusion, a rare nonsense *PTGIS* (p.E314X) variant was identified in a patient with WS with severe PPS. hPAECs with *PTGIS* p.E314X demonstrated increased viability and migration ability when compared with those harboring WT *PTGIS*, as well as reduced tube formation ability. Decreased caspase 3/7 expression was also observed in both hPAECs and hPASMCs harboring this variant. Compared with those in the healthy controls, the pulmonary artery endothelial PTGIS expression levels and urinary prostaglandin I metabolites were downregulated in the patient with PPS. Furthermore, we identified another rare *PTGIS* splice-site variant in a patient with WS with severe PPS. Based on previous reports, the 2 patients found to have *PTGIS* pathogenic variants may respond to prostaglandin I_2 drugs. This study provides important insights regarding the pathogenesis of PPS, which may inform the development of novel therapeutic strategies for PPS.

ARTICLE INFORMATION

Received January 17, 2024; accepted March 18, 2024.

Affiliations

Department of Pediatrics, Hokkaido University Hospital, Sapporo, Japan (A.C.-N., S.S., H.Y., A.M., A.T.); Department of Pediatric Cardiology and Adult Congenital Cardiology (A.C.-N., Y.F., G.H., K.I., T.N.) and Institute for Comprehensive Medical Sciences (H.A.), Tokyo Women's Medical University, Tokyo, Japan; Department of Cardiology, Peking Union Medical College Hospital, Peking Union Medical College and Chinese Academy of Medical Sciences, Beijing, China (Y.-J.M.); Department of Pediatrics, Obihiro Kosei Hospital, Obihiro, Japan (S.Y.); Department of Pediatrics, Kyushu Hospital, Japan Community Healthcare Organization, Kitakyusyu, Japan (J.M.); Department of Pediatric Cardiology, Aichi Children's Health and Medical Center, Obu, Japan (K.Y.); Division of Gene Medicine, Graduate School of Medical Science, Tokyo Women's Medical University, Tokyo, Japan (T.Y.); Department of Surgical Pathology (E.T., U.T.) and Department of Thoracic Surgery (T.K.), Hokkaido University Hospital, Sapporo, Japan; and Department of Cardiology, Guangdong Cardiovascular Institute, Guangdong Provincial People's Hospital, Guangdong Academy of Medical Sciences Southern Medical University, Guangzhou, China (Z.-C.J.).

Acknowledgments

We express our deep gratitude to the patient and the patient's family for participating in this study. Additionally, we would like to thank the medical staff of the Hokkaido University Hospital for their assistance in the collection of lung tissue and data. Furthermore, we acknowledge all volunteers who provided their urine samples for analysis.

Sources of Funding

This work was supported by the Miyata Foundation Award for Young Scientists 2021 [to A.C.N.], the CAMS Innovation Fund for Medical Sciences [2021-I2M-1-018, to Z.C.J.], National Key Research and Development Program of China [2022YFC2703902, to Z.C.J.], National High Level Hospital Clinical Research Funding [2022-PUMCH-B-099, to Z.C.J.], and Projects of National Natural Science Foundation of China [82241020, to Z.C.J.].

Disclosures

None.

Supplemental Material

Tables S1–S4
Figures S1–S8

REFERENCES

1. Chang SA, Song JS, Park TK, Yang JH, Kwon WC, Kim SR, Kim SM, Cha J, Jang SY, Cho YS, et al. Nonsyndromic peripheral pulmonary artery stenosis is associated with homozygosity of RNF213 p.Arg4810Lys regardless of co-occurrence of moyamoya disease. *Chest*. 2018;153:404–413. doi: 10.1016/j.chest.2017.09.023
2. Takahashi K, Nakamura J, Sakiyama S, Nakaya T, Sato T, Watanabe T, Ohira H, Makita K, Tomaru U, Ishizu A, et al. A histopathological report of a 16-year-old male with peripheral pulmonary artery stenosis and moyamoya disease with a homozygous RNF213 mutation. *Respir Med Case Rep*. 2020;29:100977. doi: 10.1016/j.rmcr.2019.100977
3. Cunningham JW, McElhinney DB, Gauvreau K, Bergersen L, Lacro RV, Marshall AC, Smoot L, Lock JE. Outcomes after primary transcatheter therapy in infants and young children with severe bilateral peripheral pulmonary artery stenosis. *Circ Cardiovasc Interv*. 2013;6:460–467. doi: 10.1161/CIRCINTERVENTIONS.112.000061
4. Lau EMT, Giannoulatou E, Celermajer DS, Humbert M. Epidemiology and treatment of pulmonary arterial hypertension. *Nat Rev Cardiol*. 2017;14:603–614. doi: 10.1038/nrcardio.2017.84
5. Cha SG, Song MK, Lee SY, Kim GB, Kwak JG, Kim WH, Bae EJ. Long-term cardiovascular outcome of Williams syndrome. *Congenit Heart Dis*. 2019;14:684–690. doi: 10.1111/chd.12810
6. Cuypers JA, Witsenburg M, van der Linde D, Roos-Hesselink JW. Pulmonary stenosis: update on diagnosis and therapeutic options. *Heart*. 2013;99:339–347. doi: 10.1136/heartjnl-2012-301964
7. Maegawa T, Akagawa H, Onda H, Kasuya H. Whole-exome sequencing in a Japanese multiplex family identifies new susceptibility genes for intracranial aneurysms. *PLoS One*. 2022;17:e0265359. doi: 10.1371/journal.pone.0265359
8. Yamamoto T, Shimojima K, Shimada S, Yokochi K, Yoshitomi S, Yanagihara K, Imai K, Okamoto N. Clinical impacts of genomic copy number gains at Xq28. *Human Genome Var*. 2014;1:14001. doi: 10.1038/hgv.2014.1
9. Imaizumi T, Yamamoto-Shimojima K, Yamamoto H, Yamamoto T. Establishment of a simple and rapid method to detect MECP2 duplications using digital polymerase chain reaction. *Congenit Anom*. 2020;60:10–14. doi: 10.1111/cga.12325
10. Wang XJ, Xu XQ, Sun K, Liu KQ, Li SQ, Jiang X, Zhao QH, Wang L, Peng FH, Ye J, et al. Association of rare PTGIS variants with susceptibility and pulmonary vascular response in patients with idiopathic pulmonary arterial hypertension. *JAMA Cardiol*. 2020;5:677–684. doi: 10.1001/jamacardio.2020.0479
11. Davies RJ, Holmes AM, Deighton J, Long L, Yang X, Barker L, Walker C, Budd DC, Upton PD, Morrell NW. BMP type II receptor deficiency confers resistance to growth inhibition by TGF-β in pulmonary artery smooth muscle cells: role of proinflammatory cytokines. *Am J Physiol Lung Cell Mol Physiol*. 2012;302:L604–L615. doi: 10.1152/ajplung.00309.2011
12. Pak O, Aldashev A, Welsh D, Peacock A. The effects of hypoxia on the cells of the pulmonary vasculature. *Eur Respir J*. 2007;30:364–372. doi: 10.1183/09031936.00128706
13. Catella F, Nowak J, Fitzgerald GA. Measurement of renal and non-renal eicosanoid synthesis. *Am J Med*. 1986;81:23–29. doi: 10.1016/0002-9343(86)90905-8
14. Alster P, Wennmalm A. Effect of nicotine on the formation of prostacyclin-like activity and thromboxane in rabbit aorta and platelets. *Br J Pharmacol*. 1984;81:55–60. doi: 10.1111/j.1476-5381.1984.tb10743.x
15. Goto K, Minatsuki S, Fujita K, Takeda N, Hatano M, Komuro I. Two siblings with peripheral pulmonary arterial stenosis: pulmonary angiography of advanced and early stages. *Chest*. 2022;161:e75–e80. doi: 10.1016/j.chest.2021.08.058
16. McElhinney DB, Krantz ID, Bason L, Piccoli DA, Emerick KM, Spinner NB, Goldmuntz E. Analysis of cardiovascular phenotype and genotype-phenotype correlation in individuals with a JAG1 mutation and/or Alagille syndrome. *Circulation*. 2002;106:2567–2574. doi: 10.1161/01.CIR.0000037221.45902.69
17. Lombardi A, Arseni L, Carriero R, Compe E, Botta E, Ferri D, Uggè M, Biamonti G, Peverali FA, Bione S, et al. Reduced levels of prostaglandin I2 synthase: a distinctive feature of the cancer-free trichothiodystrophy. *Proc Natl Acad Sci USA*. 2021;118:e2024502118. doi: 10.1073/pnas.2024502118
18. Nakayama T, Soma M, Watanabe Y, Hasimu B, Sato M, Aoi N, Kosuge K, Kanmatsuse K, Kokubun S, Marrow JD, et al. Splicing mutation of the prostacyclin synthase gene in a family associated with hypertension. *Biochem Biophys Res Commun*. 2002;297:1135–1139. doi: 10.1016/S0006-291X(02)02341-0
19. Huang JC, Arbab F, Tumbusch KJ, Goldsby JS, Matijevic-Aleksic N, Wu KK. Human fallopian tubes express prostacyclin (PGI) synthase and cyclooxygenases and synthesize abundant PGI. *J Clin Endocrinol Metab*. 2002;87:4361–4368. doi: 10.1210/jc.2002-020199
20. Nelson DR, Koymans L, Kamataki T, Stegeman JJ, Feyereisen R, Waxman DJ, Waterman MR, Gotoh O, Coon MJ, Estabrook RW, et al. P450 superfamily: update on new sequences, gene mapping, accession numbers and nomenclature. *Pharmacogenetics*. 1996;6:1–42. doi: 10.1097/00008571-199602000-00002
21. Wang LH, Chen L. Organization of the gene encoding human prostacyclin synthase. *Biochem Biophys Res Commun*. 1996;226:631–637. doi: 10.1006/bbrc.1996.1407
22. Ershov PV, Yablokov EO, Kaluzhskiy LA, Mezentsev YV, Ivanov AS. Prostanoid signaling in cancers: expression and regulation patterns of enzymes and receptors. *Biology*. 2022;11:590. doi: 10.3390/biology11040590
23. Lei K, Liang R, Tan B, Li L, Lyu Y, Wang K, Wang W, Wang K, Hu X, Wu D, et al. Effects of lipid metabolism-related genes PTGIS and HRASLS on phenotype, prognosis, and tumor immunity in lung squamous cell carcinoma. *Oxidative Med Cell Longev*. 2023;2023:6811625.
24. Zhuang Z, Gao C. Development of a clinical prognostic model for metabolism-related genes in squamous lung cancer and correlation analysis of immune microenvironment. *Biomed Res Int*. 2022;2022:6962056. doi: 10.1155/2022/6962056
25. Pan XY, Yang Y, Meng HW, Li HD, Chen X, Huang HM, Bu FT, Yu HX, Wang Q, Huang C, et al. DNA methylation of PTGIS enhances hepatic stellate cells activation and liver fibrogenesis. *Front Pharmacol*. 2018;9:553. doi: 10.3389/fphar.2018.00553
26. Bae SJ, Jo Y, Cho MK, Jin JS, Kim JY, Shim J, Kim YH, Park JK, Ryu D, Lee HJ, et al. Identification and analysis of novel endometriosis biomarkers via integrative bioinformatics. *Front Endocrinol*. 2022;13:942368. doi: 10.3389/fendo.2022.942368
27. Peng H, Weng L, Lei S, Hou S, Yang S, Li M, Zhao D. Hypoxia-hindered methylation of PTGIS in endometrial stromal cells accelerates endometriosis progression by inducing $CD16^-$ NK-cell differentiation. *Exp Mol Med*. 2022;54:890–905. doi: 10.1038/s12276-022-00793-1
28. Fromer M, Moran JL, Chambert K, Banks E, Bergen SE, Ruderfer DM, Handsaker RE, McCarroll SA, O'Donovan MC, Owen MJ, et al. Discovery and statistical genotyping of copy-number variation from whole-exome sequencing depth. *Am J Hum Genet*. 2012;91:597–607. doi: 10.1016/j.ajhg.2012.08.005